

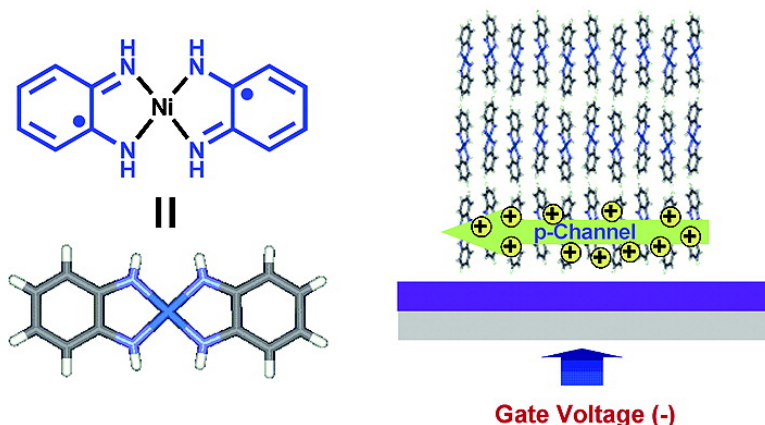
## Metal–Organic Thin-Film Transistor (MOTFT) Based on a Bis(*o*-diiminobenzosemiquinonate) Nickel(II) Complex

Shin-ichiro Noro, Ho-Chol Chang, Taishi Takenobu, Yuji Murayama, Takayoshi Kanbara, Tetsuya Aoyama, Takafumi Sassa, Tatsuo Wada, Daisuke Tanaka, Susumu Kitagawa, Yoshihiro Iwasa, Tomoyuki Akutagawa, and Takayoshi Nakamura

*J. Am. Chem. Soc.*, **2005**, 127 (28), 10012-10013 • DOI: 10.1021/ja052663s • Publication Date (Web): 23 June 2005

Downloaded from <http://pubs.acs.org> on March 25, 2009

### Metal–Organic TFT



### More About This Article

Additional resources and features associated with this article are available within the HTML version:

- Supporting Information
- Links to the 5 articles that cite this article, as of the time of this article download
- Access to high resolution figures
- Links to articles and content related to this article
- Copyright permission to reproduce figures and/or text from this article

[View the Full Text HTML](#)

## Metal–Organic Thin-Film Transistor (MOTFT) Based on a Bis(*o*-diiminobenzosemiquinonate) Nickel(II) Complex

Shin-ichiro Noro,<sup>\*,†,‡</sup> Ho-Chol Chang,<sup>\*,§,⊥</sup> Taishi Takenobu,<sup>\*,#,||</sup> Yuji Murayama,<sup>#</sup> Takayoshi Kanbara,<sup>#</sup> Tetsuya Aoyama,<sup>†</sup> Takafumi Sassa,<sup>†</sup> Tatsuo Wada,<sup>†</sup> Daisuke Tanaka,<sup>§</sup> Susumu Kitagawa,<sup>§</sup> Yoshihiro Iwasa,<sup>#,||</sup> Tomoyuki Akutagawa,<sup>‡</sup> and Takayoshi Nakamura<sup>‡</sup>

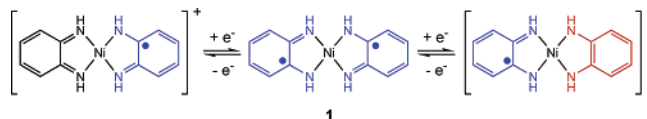
Supramolecular Science Laboratory, RIKEN (The Institute of Physical and Chemical Research), 2-1 Hirosawa, Wako-shi, Saitama 351-0198, Japan, Research Institute for Electronic Science, Hokkaido University, Sapporo 060-0812, Japan, Graduate School of Engineering, Kyoto University, Katsura, Nishikyo-ku, Kyoto 615-8510, Japan, PRESTO, Japan Science and Technology Agency, Kawaguchi, Saitama 332-0012, Japan, Institute for Materials Research, Tohoku University, Sendai 980-8577, Japan, and CREST, Japan Science and Technology Agency, Kawaguchi, Saitama 333-0012, Japan

Received April 25, 2005; E-mail: noro@es.hokudai.ac.jp; chang@sbchem.kyoto-u.ac.jp; takenobu@imr.tohoku.ac.jp

Increasing demands for inexpensive electronic components for memory, logic, and displays have recently driven research toward technologies involving organic thin-film transistors (OTFTs).<sup>1</sup> Key OTFT performance parameters, including carrier mobility, on/off current ratio, threshold voltage, and carrier type, have been optimized from two approaches: the improvement of device fabrication techniques as represented by pentacene-based OTFT,<sup>2</sup> and the development of new molecular semiconductors for active OTFT materials.<sup>1,3</sup> Although a variety of pure organic semiconductors based on acenes, oligothiophenes, C<sub>60</sub>, etc., have been extensively developed,<sup>3</sup> examples of metal–organic thin-film transistors (MOTFTs) consisting of transition metal complexes are limited to date,<sup>4</sup> despite their several advantages. (1) The ability to generate active species for charge transport through the redox activity of both the metal atom and the organic ligand. (2) Fine-tuning of the HOMO–LUMO energy gap through the interaction of the d-orbitals of the transition metal with the HOMO and/or LUMO of the ligand. (3) Diversity of the molecular framework based on the coordination number, geometry, and valence shell of the selected metal atom.

The complexes with radical *o*-semiquinonate ligands have been known to show a rich electrochemical activity. We noted bis(*o*-diiminobenzosemiquinonate) nickel(II) complex, Ni<sup>II</sup>(C<sub>6</sub>H<sub>6</sub>N<sub>2</sub>)<sub>2</sub> (**1**),<sup>5</sup> undergoes both oxidation and reduction on the radical *o*-diiminobenzosemiquinonate ligands (Scheme 1) in solution state.<sup>5a</sup> The

### Scheme 1



electrochemical measurement of **1** (1 mM) was conducted in 0.1 M (*n*-Bu<sub>4</sub>N)(BF<sub>4</sub>)/DMF solution. The voltammograms showed a reversible one-electron oxidation and a reversible one-electron reduction at  $E_{1/2} = -0.36$  and  $-1.37$  V versus the ferrocene/ferrocenium couple, respectively. The HOMO–LUMO energy gap obtained from the redox peaks is 1.01 eV.<sup>6</sup> The absorption edge in the UV–vis–NIR spectra measured in DMF solution also afforded the HOMO–LUMO energy gap of 1.03 eV, whose value is

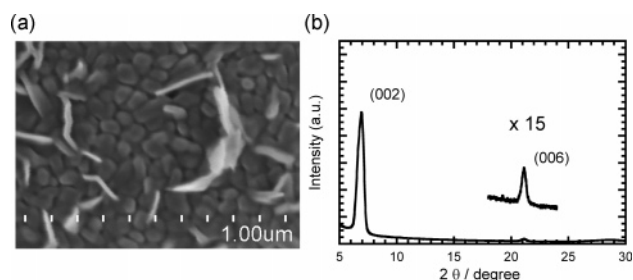


**Figure 1.** (a) SEM image and (b) out-of-plane XRD pattern of the film of **1** evaporated on a SiO<sub>2</sub>.

consistent with the result from the electrochemical measurement. Despite its interesting electrochemical activity, the application to thin-film devices containing TFTs is scarcely reported to date. In this communication, we describe the preparation, vacuum deposition, structure, and properties of MOTFT formed by **1**.

The films of **1** (50–100 nm thickness) were grown by vacuum deposition at a base pressure of 10<sup>−6</sup> Torr during deposition at room temperature. The SEM image of the film on SiO<sub>2</sub> (Figure 1a) revealed that vacuum deposition of **1** afforded a uniform film characterized by highly interconnected grains (~100 nm).<sup>7</sup> UV–vis–NIR spectra of a vacuum deposition film of **1** on quartz showed an absorption edge of 1500–1600 nm, which indicates the formation of a densely assembled structure with a band gap of ca. 0.80 eV. These results clearly point out that the film of **1** is a good candidate for the semiconducting layer of TFT devices.

The single crystal of **1** has been previously reported.<sup>8</sup> The structure shows two-dimensional layers with a herringbone-type arrangement through CH– $\pi$  interactions in the *ab* plane stack along the *c*-axis with a period of ca. 12.6 Å. The molecular orientation within the film was evaluated using the XRD measurements. The out-of-plane XRD pattern (Figure 1b) of the film on SiO<sub>2</sub> indicated a sharp peak at 6.86° corresponding to the (002) plane with a *d* spacing of ca. 12.9 Å normal to the substrate surface. The sharp diffraction peak and the existence of a higher-order peak corresponding to the (006) plane illustrate the high degree of crystallinity in the film. However, the in-plane XRD pattern was distinctly different from the out-of-plane one; several peaks which indexed as (*hkl*) planes were observed. These results indicate (1) molecular assembly similar to that in the single crystal, (2) uniaxial orientation of the film normal to the substrate surface, and (3) conduction channels parallel to the substrate surface.

The molecular orientation within the film was also estimated using polarized electronic absorption spectra, and the transmission

<sup>†</sup> RIKEN.  
<sup>‡</sup> Hokkaido University.  
<sup>§</sup> Kyoto University.  
<sup>⊥</sup> PRESTO.  
<sup>#</sup> Tohoku University.  
<sup>||</sup> CREST.

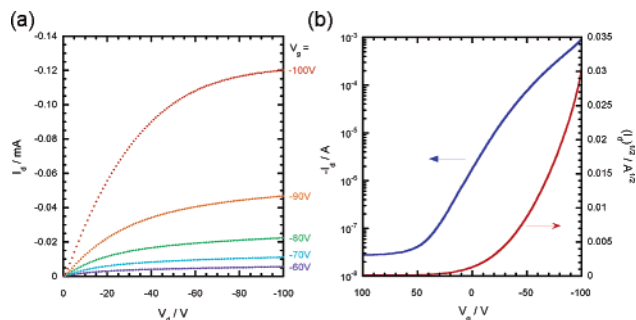


**Figure 2.** (a) Plots of drain current ( $I_d$ ) versus drain voltage ( $V_d$ ) for various applied gate voltage ( $V_g$ ) in MOTFT of **1**. (b) Plots of  $I_d$  and  $I_d^{1/2}$  versus  $V_g$  at  $V_d = -100$  V for the same device.  $L = 30$   $\mu\text{m}$  and  $W = 38.9$  nm.

( $T$ ), and reflection–absorption ( $RA$ ) IR spectra. The polarized UV–vis–NIR spectra of the film of **1** did not indicate any in-plane anisotropy with the normal incidence, which means the isotropy of molecules within the substrate surface. The use of p- and s-polarized lights at the incident angle of  $45^\circ$  demonstrated that the absorption intensity at 526 nm for the p-polarization is larger than that of the s-polarization ( $A_{p45}/A_{s45}$  ratio  $\approx 2.4$ ). This difference in absorption can be accounted for by the largely perpendicular orientation of the intramolecular transition moment to the substrate surface. These results are in good agreement with those from XRD. The  $T$ - and  $RA$ -IR spectra in the region of the  $\nu_{\text{NH}}$  bands ( $3300$ – $3325$   $\text{cm}^{-1}$ ) also agreed with the results of the molecular orientation similar to the XRD and the UV–vis–NIR spectra.<sup>9</sup>

We fabricated a MOTFT device of **1** with a bottom contact configuration. A heavily doped  $n$ -type Si wafer was used for the back gate electrode with a 400 nm insulating layer of thermally grown  $\text{SiO}_2$  on top of it. Drain and source electrodes (10/100 nm Ti/Au) were fabricated on the surface of the  $\text{SiO}_2$  layer. The device had a channel length ( $L$ ) of 30  $\mu\text{m}$  and a width ( $W$ ) of 38.9 nm. During the deposition of **1**, the substrate temperature was kept at room temperature. This device was stable and, therefore, was characterized in the atmosphere. Figure 2a displays a plot of drain current ( $I_d$ ) as a function of drain voltages ( $V_d$ ) for various applied gate voltages ( $V_g$ ). The semiconductor layer of **1** acted as a p-channel.  $I_d$  increased almost linearly with  $V_d$ , followed by saturation due to the pinch off of the accumulation layer. Figure 2b shows the relation between  $I_d$  and  $V_g$  at  $V_d = -100$  V for the same device. The left-hand side scale indicates an on/off ratio of  $3 \times 10^4$ . The hole mobility,  $\mu$ , and the threshold voltage,  $V_{\text{th}}$ , extracted from the saturated region were  $3.8 \times 10^{-2}$   $\text{cm}^2/\text{Vs}$  and  $-42$  V, respectively. This  $\mu$  value is larger than those of MOTFTs with metallophthalocyanines deposited on unheated substrates.<sup>4f–h,k</sup>

Note that the reduction potential of **1** is similar to those of perfluoropentacene and  $\text{C}_{60}$  observed at  $E_{1/2} = -1.13$  and  $-1.14$  V versus ferrocene/ferrocenium couple, respectively, which are known as excellent  $n$ -type semiconductors for OTFTs.<sup>3c,g,h</sup> In addition, the HOMO–LUMO gap is considerably smaller than that of quinoidal terthiophene, which shows ambipolar OTFT ability.<sup>3d</sup> Therefore, we expect that the ambipolar MOTFT with **1** could be achieved by utilization of electrodes with small work functions and/or slight lowering of LUMO level by chemical modifications.

In summary, we succeeded in the formation of semiconductor film of metal complex **1** as a MOTFT. The obtained film had uniaxial orientation structure along the normal to the substrate and showed good p-type TFT character. Although complexes with radical  $o$ -semiquinonate are well-known to show both reduction and oxidation with a narrow HOMO–LUMO gap,<sup>5a,6,10</sup> their utilization as a semiconducting layer for TFT, to date, is scarcely reported at all. To the best of our knowledge, this study is the first

report of a complex with radical  $o$ -semiquinonate ligands being used as the conducting layer of TFT device. Further studies on controlling of the assembling structure and fine HOMO–LUMO tuning by the modification of **1** (exchange of metal ion, introduction of substituents, and expansion of  $\pi$ -conjugation) are being carried out in order to obtain not only high-performance but also ambipolar MOTFTs.

**Acknowledgment.** The authors thank Dr. D. Hashizume (RIKEN) for measuring the in-plane XRD. S.N. expresses gratitude to RIKEN for supporting him under a Special Postdoctoral Researchers Program.

**Supporting Information Available:** Experimental procedures, results of cyclic voltammograms, in-plane XRD, UV–vis–NIR spectra in solution and film state, polarized UV–vis–NIR spectra, and  $T$ - and  $RA$ -IR spectra (PDF). This material is available free of charge via the Internet at <http://pubs.acs.org>.

## References

- (1) (a) Dimitrakopoulou, C. D.; Malenfant, P. R. R. *Adv. Mater.* **2002**, *14*, 99–117. (b) Horowitz, G. *Adv. Mater.* **1998**, *10*, 365–377. (c) Katz, H. E.; Bao, Z.; Gilat, S. L. *Acc. Chem. Res.* **2001**, *34*, 359–369.
- (2) (a) Lin, Y. Y.; Gundlach, D. J.; Nelson, S. F.; Jackson, T. N. *IEEE Electron Device Lett.* **1997**, *18*, 606–608. (b) Lin, Y. Y.; Gundlach, D. J.; Nelson, S. F.; Jackson, T. N. *IEEE Trans. Electron Devices* **1997**, *45*, 1325–1331. (c) Knipp, D.; Street, R. A.; Völkel, A.; Ho, J. J. *J. Appl. Phys.* **2003**, *93*, 347–355. (d) Halik, M.; Klauk, H.; Zschieschang, U.; Schmid, G.; Dehm, C.; Schütz, M.; Maisch, S.; Effenberger, F.; Brunnbauer, M.; Stellacci, F. *Nature* **2004**, *431*, 963–966. (e) Kobayashi, S.; Nishikawa, T.; Takenobu, T.; Mori, S.; Shimoda, T.; Mitani, T.; Shimotani, H.; Yoshimoto, N.; Ogawa, S.; Iwasa, Y. *Nat. Mater.* **2004**, *3*, 317–322.
- (3) (a) Moon, H.; Zeis, R.; Borkent, E.-J.; Besnard, C.; Lovinger, A. J.; Siegrist, T.; Kloc, C.; Bao, Z. *J. Am. Chem. Soc.* **2004**, *126*, 15322–15323. (b) Ong, B. S.; Wu, Y.; Liu, P.; Gardner, S. *J. Am. Chem. Soc.* **2004**, *126*, 3378–3379. (c) Kobayashi, S.; Takenobu, T.; Mori, S.; Fujiwara, A.; Iwasa, Y. *Appl. Phys. Lett.* **2003**, *82*, 4581–4583. (d) Chesterfield, R. J.; Newman, C. R.; Pappenfus, T. M.; Ewbank, P. C.; Haukaas, M. H.; Mann, K. R.; Miller, L. L.; Frisbie, C. D. *Adv. Mater.* **2003**, *15*, 1278–1282. (e) Facchetti, A.; Mushrush, M.; Katz, H. E.; Marks, T. N. *J. Am. Chem. Soc.* **2003**, *125*, 33–38. (f) Takimiya, K.; Kunugi, Y.; Konda, Y.; Niihara, N.; Otsubo, T. *J. Am. Chem. Soc.* **2004**, *126*, 5084–5085. (g) Sakamoto, Y.; Suzuki, T.; Kobayashi, M.; Gao, Y.; Fukai, Y.; Inoue, Y.; Sato, F.; Tokito, S. *J. Am. Chem. Soc.* **2004**, *126*, 8138–8140. (h) Haddon, R. C.; Perel, A. S.; Morris, R. C.; Palstra, T. T. M.; Hebard, A. F. *Appl. Phys. Lett.* **1995**, *67*, 121–123.
- (4) (a) Ohta, H.; Kambayashi, T.; Nomura, K.; Hirano, M.; Ishikawa, K.; Takezoe, H.; Hosono, H. *Adv. Mater.* **2004**, *16*, 312–316. (b) Xiao, K.; Liu, Y.; Huang, X.; Xu, Y.; Yu, G.; Zhu, D. *J. Phys. Chem. B* **2003**, *107*, 9226–9230. (c) Noh, Y.-Y.; Kim, J.-J.; Yoshida, Y.; Yase, K. *Adv. Mater.* **2003**, *15*, 699–702. (d) Pearson, C.; Moore, A. J.; Gibson, J. E.; Bryce, M. R.; Petty, M. C. *Thin Solid Films* **1994**, *244*, 932–935. (e) Caseri, W. R.; Chanzy, H. D.; Feldman, K.; Fontana, M.; Smith, P.; Tervoort, T. A.; Goossens, J. G. P.; Meijer, E. W.; Schenning, A. P. H. J.; Dolbnya, I. P.; Debije, M. G.; de Haas, M. P.; Warman, J. M.; van de Craats, A. M.; Friend, R. H.; Siringhaus, H.; Stutzmann, N. *Adv. Mater.* **2003**, *15*, 125–129. (f) Bao, Z.; Lovinger, A. J.; Dodabalapur, A. *Adv. Mater.* **1997**, *9*, 42–44. (g) Hoshino, S.; Kamata, T.; Yase, K. *J. Appl. Phys.* **2002**, *92*, 6028–6032. (h) Guillaud, G.; Sadoun, M. A.; Maitrot, M.; Simon, J.; Bouvet, M. *Chem. Phys. Lett.* **1990**, *167*, 503–506. (i) Guillaud, G.; Simon, J.; Germain, J. P. *Coord. Chem. Rev.* **1998**, *178–180*, 1433–1484. (j) Tada, H.; Touda, H.; Takada, M.; Matsushige, K. *Appl. Phys. Lett.* **2000**, *76*, 873–875. (k) Guillaud, G.; Chaabane, B.; Jouve, C.; Gamoudi, M. *Thin Solid Films* **1995**, *258*, 279–282.
- (5) (a) Balch, A. L.; Holm, R. H. *J. Am. Chem. Soc.* **1966**, *88*, 5201–5209. (b) Mederos, A.; Domínguez, S.; Hernández-Mokina, R.; Sanchiz, J.; Brito, F. *Coord. Chem. Rev.* **1999**, *193–195*, 913–939.
- (6) Herebian, D.; Wiegardt, K. H.; Neese, F. *J. Am. Chem. Soc.* **2003**, *125*, 10997–11005.
- (7) On the surface, another grain with a flakelike shape was formed. However, the film is so thick (50–100 nm) that the flakelike grains scarcely affect the TFT character.
- (8) Hall, G. S.; Soderberg, R. H. *Inorg. Chem.* **1968**, *7*, 2300–2303.
- (9) Umemura, J.; Kamata, T.; Kawai, T.; Takenaka, T. *J. Phys. Chem.* **1990**, *94*, 62–67.
- (10) (a) Pierpont, C. G.; Lange, C. W. *Prog. Inorg. Chem.* **1994**, *41*, 331–342. (b) Chang, H.-C.; Ishii, T.; Kondo, M.; Kitagawa, S. *J. Chem. Soc., Dalton Trans.* **1999**, 2467–2476. (c) Herebian, D.; Bothe, E.; Neese, F.; Weyhermüller, T.; Wiegardt, K. *J. Am. Chem. Soc.* **2003**, *125*, 9116–9128.

JA052663S